Structural characterization and *in vitro* bioactivity assessment of SiO_2–CaO–P_2O_5–K_2O–Al_2O_3 glass as bioactive ceramic material

4.1 Introduction

Bioactive glasses belong to an elite class of biomaterials which are generally based on amorphous silicate compounds (Huygh *et al*., 2002). It is well known that these materials are able to bind with the bones in living organisms and have been clinically used as dental and orthopedic implants (Schepers *et al*., 1991). The first bioactive glass was invented by Hench which was known as 45S5 Bioglass® (Jones, 2013). The author made a degradable glass in the Na_2O–CaO–SiO_2–P_2O_5 system which was rich in CaO content and the composition of this was close to a ternary Na_2O–CaO–SiO_2 system (Hench, 2006 and Hench *et al*., 1971). This launched the field of bioactive ceramics with several new materials which were formed from the compositional variations on bioactive glasses (Hench, 2006), glass–ceramics (Kokubo, 1991) as well as ceramics (LeGeros, 2002). Bioglass® (45S5) bonds with bone rapidly and also stimulates bone growth away from the bone implant interface. The mechanism for bone bonding is attributed due to formation of hydroxy carbonate apatite (HCA) layer on the surface of the glass followed by initial glass dissolution (Hench *et al*., 1971). HCA is similar to bone mineral and was believed to interact with collagen fibrils which bonds with the host bone. The osteogenic properties of the glass were considered to be due to the dissolution products of the glass (Hench *et al*., 2002). However, its relatively low strength and brittleness limit its application to non-load bearing conditions (Cao *et al*., 1996). The addition of elements

such as magnesium, aluminum, zirconium and titanium may be used to control some physico-chemical and mechanical properties of bioglasses (Agathopoulos *et al*., 1996 and Marti, 2000). Many systematic investigations have been carried out by earlier workers (El-Kheshen *et al*., 2008, Sitarz *et al*., 2010 and Sitarz 2010) in order to see the effect of alumina on bioactivity and mechanical properties of phosphate, silicate and phospho–silicate bioactive glasses and glass–ceramics. It was mentioned earlier that the addition of Al_2O_3 in the bioactive glass had improved the repair in bone defect and controlled the degradation rate for long-term stability of the implants (Lashneva *et al*., 1998). Sitarz *et al*. (Sitarz *et al*., 2010) had observed that the addition of Al^{3+} in proper concentration increased the mechanical resistance of the bioglasses. The presence of Al_2O_3 has resulted the breaking of P=O bonds and the Si–O–P linkages were replaced by Al–O–P linkages in the glass network which prevented the degradation of $KCaPO_4$–SiO_2 and $KCaPO_4$–SiO_2–$AlPO_4$ systems (Sitarz, 2010). However, the addition of alumina in higher concentrations in the borate free silicate-based bioactive glass is quite undesirable due to the ability to damage the genome or to disrupt the cellular metabolic processes and harmful impact on the bioactivity of glasses (Anderson, 1990 and Gross *et al*., 1985). It was reported that the potash based bioactive glass had shown better biocompatibility than soda based bioactive glass. However, the role of Al_2O_3 for K_2O in the past has never been investigated in such systems. The incorporation of K_2O has been shown to be useful in bioactive glasses without influencing their bioactivity and thermo-mechanical properties (Cannillo *et al*., 2009). The potassium ions having various sizes influence the structure of bioactive glasses having made the system more compact and there by affect the mechanical properties of the glass (Tylkowski, *et al*., 2013). So, the aim of this work is to

provide information on the effect of Al_2O_3 substitution in potash based bioactive glass by introducing alumina from 0.5–2.5 mol% into it. Therefore, in the present investigation, the concentration of K_2O was varied with molar addition of Al_2O_3 from 0.5% to 2.5%. The idea for assessment of *in vitro* bioactivity in simulated body fluid (SBF), physico-chemical, mechanical properties as well as cell culture of the glasses has been also mooted out. It is expected that the bioactivity and physico-mechanical properties would be improved significantly with increasing the concentration of Al_2O_3 in the base bioactive glass. Furthermore, we have extensively investigated the *in vitro* cell culture studies, like cell viability, cytotoxicity, proliferation, apoptosis and cell attachment for better conclusions. Interestingly, all the samples are tolerant to white blood cells (WBC) and RBC causing no significant loss of viability or hemolysis.

4.2 Materials and methods

4.2.1 Sample preparation

Glass samples were prepared in five different compositions by taking the starting materials as reagent grade fine-grained quartz (SiO_2), calcium carbonate ($CaCO_3$), ammonium dihydrogen phosphate ($(NH_4)H_2PO_4$), potassium carbonate (K_2CO_3) in the required stoichiometric ratio in mol% (Table 4.1). The required amounts of analytical reagent grade Al_2O_3 were added in the batch for the partial substitution of K_2O. The raw materials for different samples were properly weighed. The mixing of different batches was done for 30 min and then after that, they were melted in a 100 ml platinum-2% rhodium crucible for 4h kept in a globar electric furnace at 1400°C in air atmosphere. The temperature of the furnace was controlled with in ± 10°C by an automatic temperature

indicator-cum-controller. Further, the glass melt was taken out of the furnace, poured on an aluminum sheet in a rectangular mold and transferred immediately to an annealing furnace. The glass samples were properly annealed at 500°C for 1h and cooled slowly to room temperature with a controlled rate of cooling inside the muffle furnace to remove the stress and strain from the glass. A part of the annealed bioactive glass samples was cut, ground and polished for measurement of its physical and mechanical properties.

Table 4.1 Mol% compositions of the bioactive glass samples.

Sl. No.	SAMPLE	SiO_2	CaO	P_2O_5	K_2O	Al_2O_3	Al_2O_3 / K_2O ratio
1.	K1	42	34	6	18	0	0.00
2.	K2	42	34	6	17.5	0.5	0.028
3.	K3	42	34	6	17	1.0	0.058
4.	K4	42	34	6	16.5	1.5	0.090
5.	K5	42	34	6	15.5	2.5	0.161

The other parts of the samples were crushed in a pestle mortar and then ground in an agate mortar to make fine powders for measurements of its bioactivity and other properties with various experimental techniques such as XRD, FTIR spectrometry, SEM analysis and pH measurements. The *in vitro* cell culture studies were also performed with the bioactive glass samples against human osteosarcoma cells U2-OS.

4.2.3 X-ray diffraction (XRD)

The powdered samples were subjected to X-ray diffraction analysis using a Rigaku portable XRD machine (Rigaku, Tokyo, Japan) (40kV, 20 mA) from 20° to 80° in steps

of 0.018. The Cu Kα radiation with Ni filtered is used for X-ray analysis. Phase identification was carried out by comparing the XRD patterns of the bioactive glass samples with the standard database stated by JCPDF X-ray diffraction card files.

4.3 Results and discussion

4.3.1 Mechanical properties

4.3.1.1 Density and compressive strength

Figs. 4.1 and 4.2 show the density and compressive strength of the glass samples as a function of Al_2O_3/K_2O ratio within error bars. From Figs. 4.1 and 4.2 it is clear that an increase in Al_2O_3/ K_2O ratio with increasing Al_2O_3 substitution resulted an increase in the density and the compressive strength of glass samples from 2.74 to 2.79 gm/cc and 58 to 69 MPa respectively.

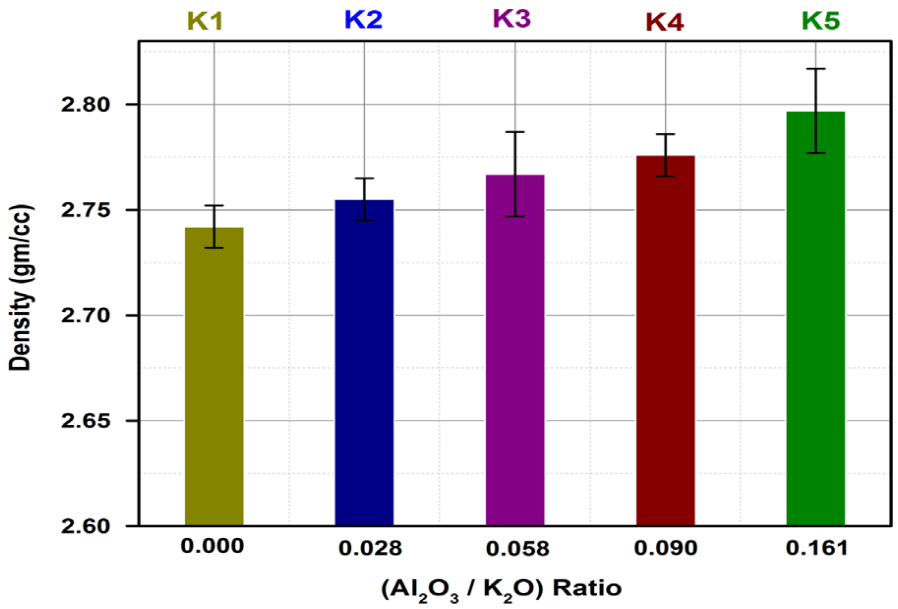

Fig. 4.1: Variation in density with Al_2O_3/K_2O ratio in bioactive glass samples (K1–K5).

This is attributed due to the reason that the aluminum ions might have occupied interstitial sites within the glass network (Muller *et al*., 1983 and Brow *et al*., 1997). Therefore, it increased the densities and resulted in creating new bonds with incorporation of aluminum ions in the bioactive glasses. It has caused reinforcement of glass structure and resulted in improvement in the compression of the glass samples.

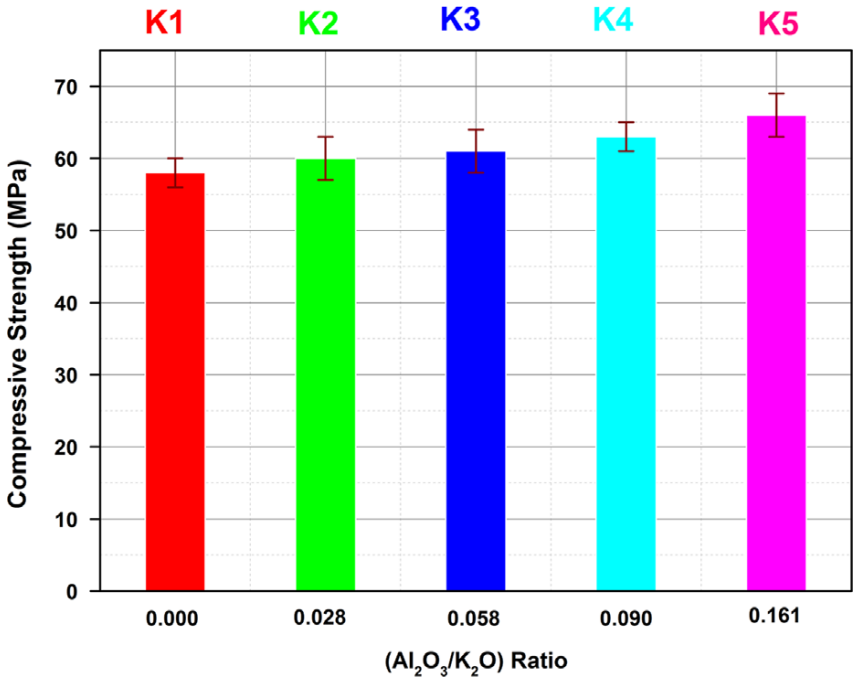

Fig. 4.2: Variation in compressive strength with Al_2O_3/K_2O ratio in bioactive glass samples (K1–K5).

2.3.1.2 Elastic modulus, shear modulus and bulk modulus

Fig. 3 represents the experimental values of elastic moduli such as Young's modulus (E), shear modulus (S) and bulk modulus (K) of the bioactive glass samples with increasing Al_2O_3/K_2O ratio. All the elastic moduli values were found to increase with increasing Al_2O_3/K_2O ratio. The elastic moduli of the bioactive glass samples show similar trends

regarding improvement in their mechanical properties with the variation in the ultrasonic velocities. The elastic modulus of alkali silicate glasses was normally found to increase with increasing concentration of modifier above a critical limit as a result of an increase in cohesion (Lin *et al*., 2006).

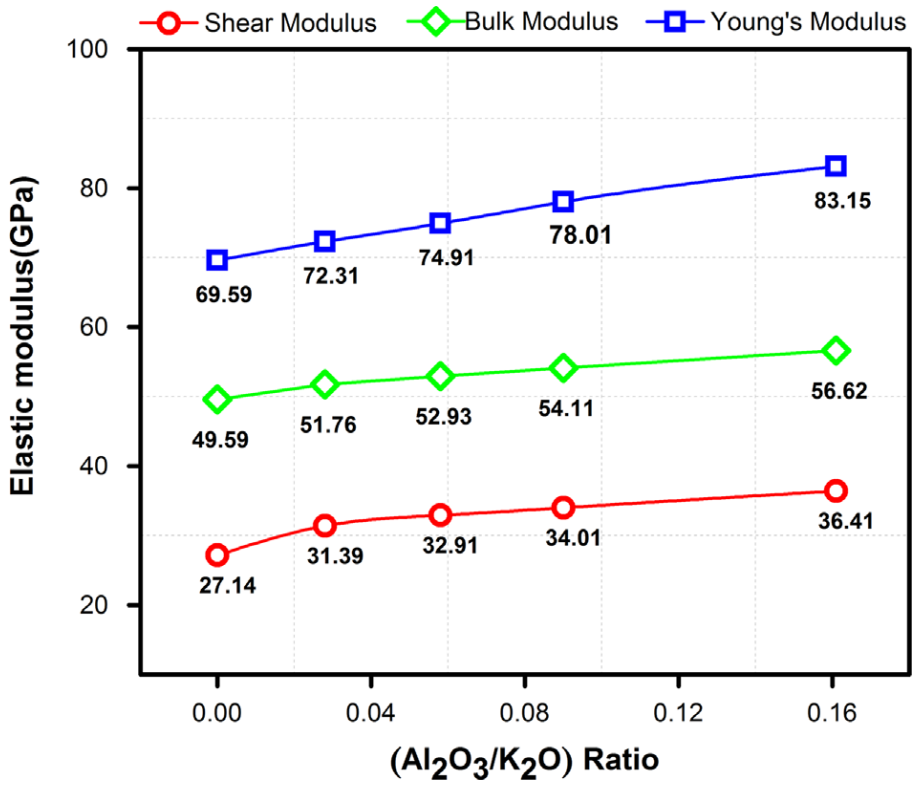

Fig. 4.3: Elastic modulus, shear modulus and bulk modulus of all bioactive glass samples (K1-K5).

Thus, a greater bulk modulus of the glass samples can be partially attributed due to addition of more amounts of modifiers like K_2O and CaO in the silicate glass samples. The authors have further mentioned that the effect of P_2O_5 on the elasticity of their glasses was not clear, although phosphorus has caused a more polymerized silicate network. Hench (Hench, 1998) has pointed out that the Young's modulus of cortical bone

is about 7–30 GPa which is far below the most ceramic based implants. Hence, from the point of view of biomechanical compatibility, the SiO_2–CaO–P_2O_5–K_2O– Al_2O_3 bioactive glass samples have been found to be better. It was also known that the glasses and ceramics are brittle materials, as a consequence of which their handling and mechanical properties are not adequate for significant load bearing applications. Therefore, a bioactive glass having elastic modulus higher than that of bone is required for clinical applications. So, there was an increase in Young's modulus from 69.59 to 83.15GPa with increasing Al_2O_3 content in the present base bioactive glass. Similar results were also obtained for shear and bulk moduli which showed improvement in the mechanical properties of bioactive glasses with varying ultrasonic velocities.

4.3.2. pH behavior

Fig. 4.4 shows the variation of pH of bioactive glass samples after immersing in SBF solution up to 28 days. It shows that for all bioactive glass samples, the pH increases within 1 to 7 days as compared to the initial pH of the SBF solution at 7.4 and 37°C temperature under physiological condition. The increase in pH values is due to fast release of cations through exchange with H^+ or H_3O^+ ions in the SBF solution. The H^+ ions are being replaced by cations which cause an increase in hydroxyl concentration of the solution. This leads to attack on the silica glass network, which results silanols formation leading to decrease in pH as indicated in Fig. 4.4 when bioactive glass samples were immersed in SBF solution for 7 to 28 days. It was also seen that the decrease in the pH of the SBF solution after 14 days was due to breaking of glass network. Fig. 4.4 shows that addition of alumina up to 1.5 mol%, results an increase in pH of the SBF solution containing immersed samples which attained maxima after around three days

and then it decreased with time referring to base glass sample. However, the addition of Al_2O_3 beyond this (> 1.5–2.5 mol%) up to 2.5 mol% caused a decrease in maxima of the pH of the SBF solution containing immersed sample. This dictates that addition of Al_2O_3 up to 1.5 mol% in the glass samples has increased its bioactivity, but beyond 1.5 mol% up to 2.5 mol% of Al_2O_3 retards the bioactivity of the glass samples (Fig. 4.4). This observation can be explained in the manner that addition of Al_2O_3 up to 1.5 mol% goes into formation of AlO_6 octahedra and produces more of non-bridging oxygens which results in an increase in bioactivity of samples.

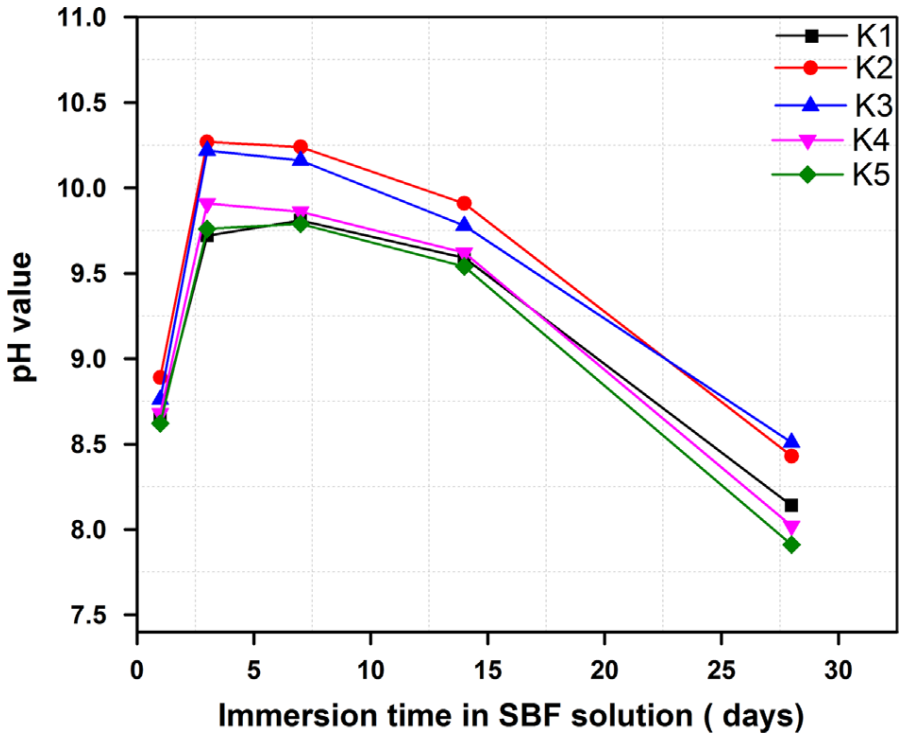

Fig. 4.4: Variation of pH of bioactive glass samples (K1-K5) after immersing in simulated body fluid (SBF) up to 28 days at 37°C temperature.

Whereas further addition of Al_2O_3 beyond 1.5 mol%, results in the formation of AlO_4 tetrahedra which causes a decrease in the bioactivity of the samples (Belkebir *et al.*,

1999, Zhao *et al*., 2009 and Brow *et al*., 1997). Greenspan *et al*. (Greenspan *et al*., 1976) also confirmed that the change in pH of glass samples took place after immersion in SBF solution. Morphological properties of bioactive glasses also indicate that soaking in SBF solution leads to formation of hydroxy apatite layer on the surface of the samples (Hayakawa *et al*., 1999 and Kasuga *et al*., 2001). The maxima of pH values were recorded on the third days as pH 9.81, 10.24, 10.16, 9.86 and 9.79 for the samples K1–K5 respectively at 37°C under physiological condition, which is due to the fast dissolution rate. On the addition of Al_2O_3 up to 1.5 mol%, the maxima of pH is more than the base glass, but beyond that it is lower than the base glass sample.

The high degradation rate leads to higher pH value. So, an increase in the pH value of SBF solution also favors the hydroxy carbonate apatite formation. When bone is formed, the cross-linking of the collagen chains and the subsequent precipitation of hydroxyl carbonate apatite is pH dependent and require a high pH at the bone formation site (Chengtie *et al*., 2007). Ohtsuki and Kokubo (Ohtsuki *et al*., 1992) had earlier investigated the effect of Al_2O_3 on bioactivity of $CaO–SiO_2–Al_2O_3$ glasses by *in vitro* tests. They evaluated the bioactivity of the glass samples by hydroxy apatite formation on the surface of these glasses using various instrumental techniques and found that calcium alumino-silicate containing less than 1.5 mol% Al_2O_3 formed the apatite layer on the surface of the glass, but glasses containing more than 1.7 mol% of Al_2O_3 did not form this layer. The results of the present investigations entirely based on the well established *in vitro* tests are well supported by earlier studies (Hayakawa *et al*., 1999, Kasuga *et al*., 2001 and Ohtsuki *et al*., 1992).

4.3.3 SEM analysis of bioactive glass samples

The SEM micrographs of bioactive glass samples before soaking in SBF solution are shown in Fig. 4.5(a)–(e) which shows different rod type structures and irregular grains of bioactive glass samples which are quite similar to the results observed by Hanan *et al*. (Hanan *et al*., 2009).

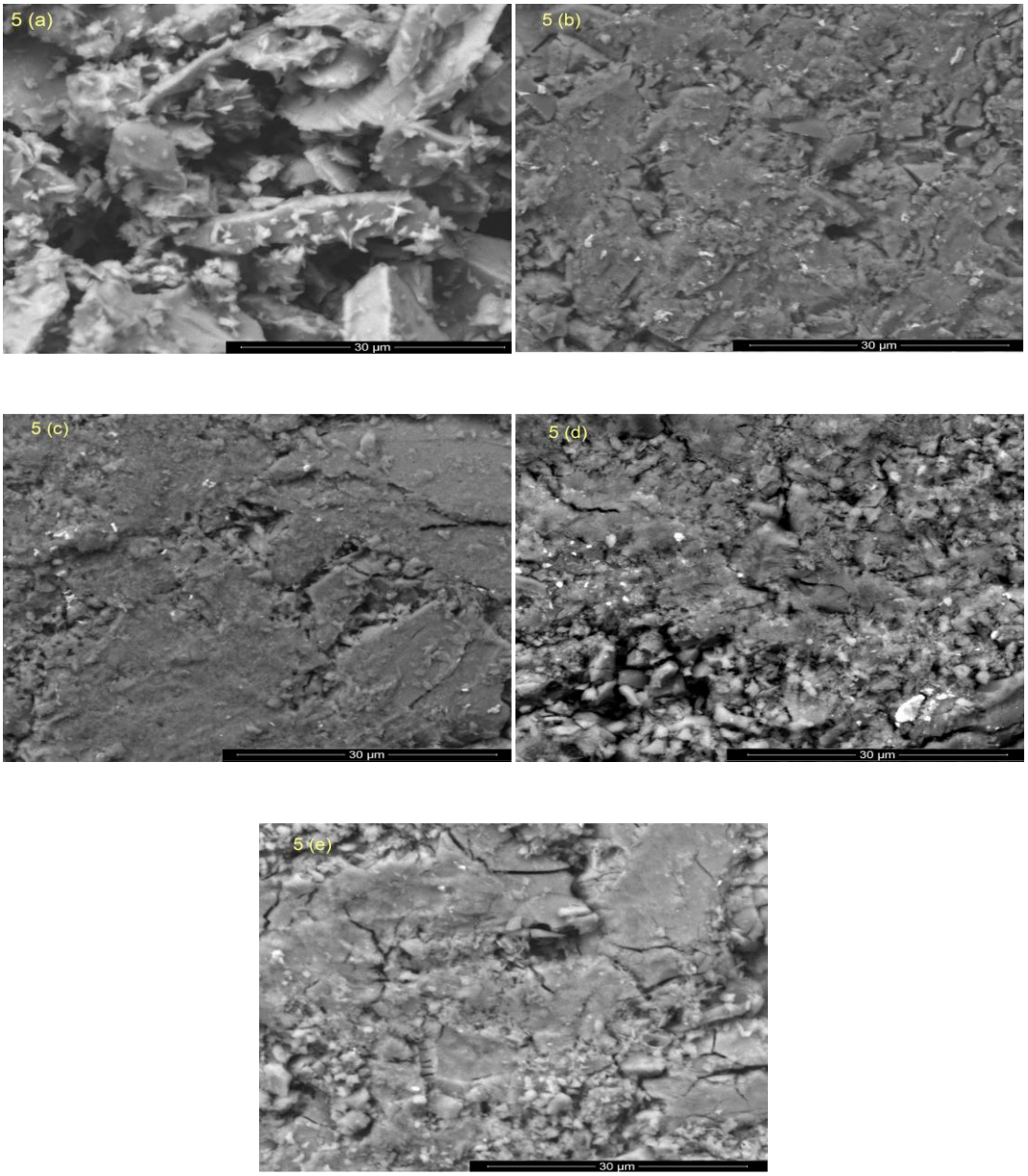

Fig. 4.5 (a–e): SEM micrographs of bioactive glass samples (K1-K5) before soaking in SBF solution.

Fig. 4.6(a)–(e) shows the SEM micrographs of bioactive glass samples after soaking in SBF solution for 28 days. It is clear from Fig. 4.6 (a-e) that bioactive glass samples which were soaked in SBF solution for 28 days were covered with irregular shape of carbonated hydroxy apatite and grounded HCA particles have grown into several agglomerates.

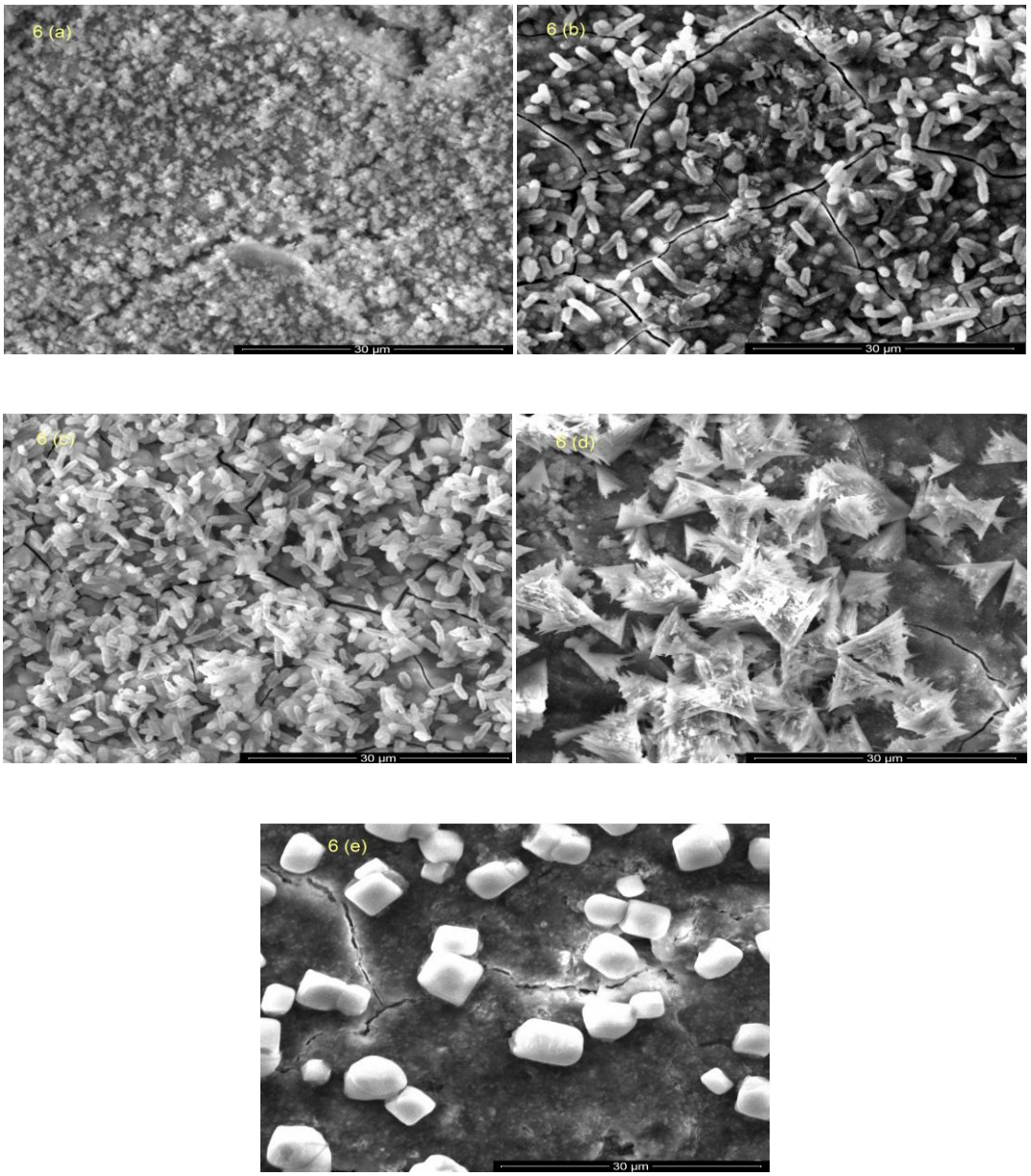

Fig. 4.6(a–e): SEM micrographs of bioactive glass samples (K1-K5) which were soaked in SBF solution for 28 days.

On SBF treatment HCA clusters change in a finer structure after 28 days of soaking due to partial dissolution and re-precipitation phenomena in solution. This happens due to solution refreshing and demonstrating the formation of a continuous layer of HCA (Verne *et al*., 2005). So, after comparing these micrographs it can be concluded that the micrographs show the formation of HCA on the surface of bioactive glass samples after immersion in SBF solution for 28days.

4.3.4 *In vitro* bioactivity of bioactive glasses by X-ray difractometry

Fig. 4.7 shows the XRD patterns of the bioactive glass samples before soaking them into the SBF. Before being soaked in SBF solutions, there was no XRD peak for the bioactive glass samples, except a hump like peak ranging from 20° to 30° as it is attributed due to Si–O–Si network.

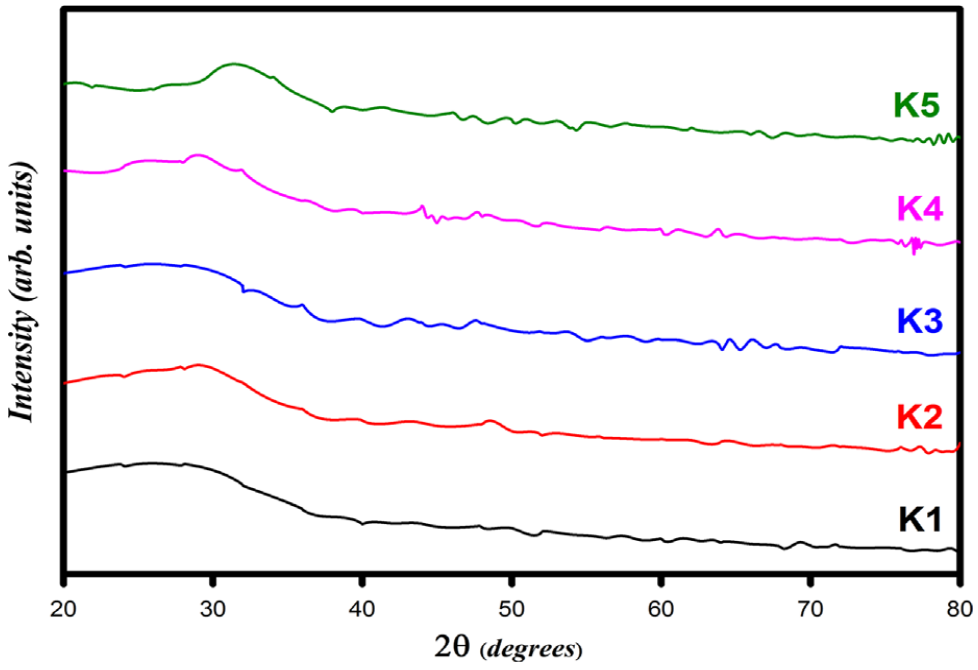

Fig. 4.7: XRD patterns of the bioactive glass samples (K1-K5) before soaking them into the simulated body fluid (SBF) solution.

So, it is clear that bioactive glass samples were amorphous in nature before being soaked in SBF solution (Brovarone *et al*., 2006). Fig. 4.8 shows the XRD patterns of the bioactive glass samples soaked in the SBF solution for 28 days. After SBF treatment for 28 days, the diffraction pattern of all bioactive glass samples shows two sharp peaks at 32.8° and 31.7° which is due to the presence of calcium phosphate hydroxide matched with PDF no.831886. These two peaks are regarded as crystalline nature of HCA nucleated from the solution (Fujiabayashi *et al*., 2003 and Kokubo *et al*., 2003). Therefore, this present system favours the HCA formation which has been also proved by the SEM and FTIR spectrometry as shown in Fig. 4.6 and next Figs. 4.9–4.13, respectively.

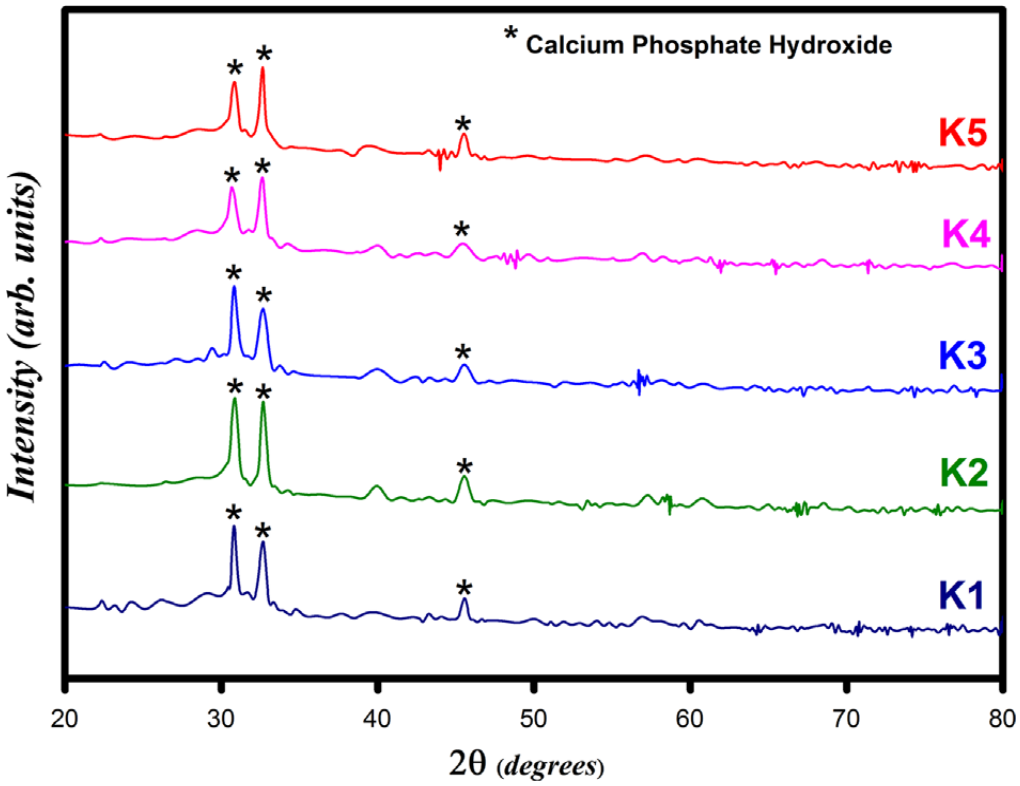

Fig. 4.8: XRD patterns of the bioactive glass samples (K1-K5) soaked in the simulated body fluid (SBF) solution for 28 days.

4.3.5 FTIR-spectrometry

Figs. 4.9–4.13 show the FTIR spectral absorption bands in the bioactive glasses before and after immersion in SBF for different time periods such as 1, 3, 7, 14 and 28 days. In general, it is well known that an increase in the intensity of absorption bands indicates an increase in molecular concentration of species formed at surface of the bioactive glass treated with SBF solution progressively with increasing soaking time. The present results obtained by FTIR spectrometry were also in good agreement with the earlier studies made by previous workers (Kim *et al*., 1989, Filguei ras *et al*., 1993 and Rehman *et al*., 2000).

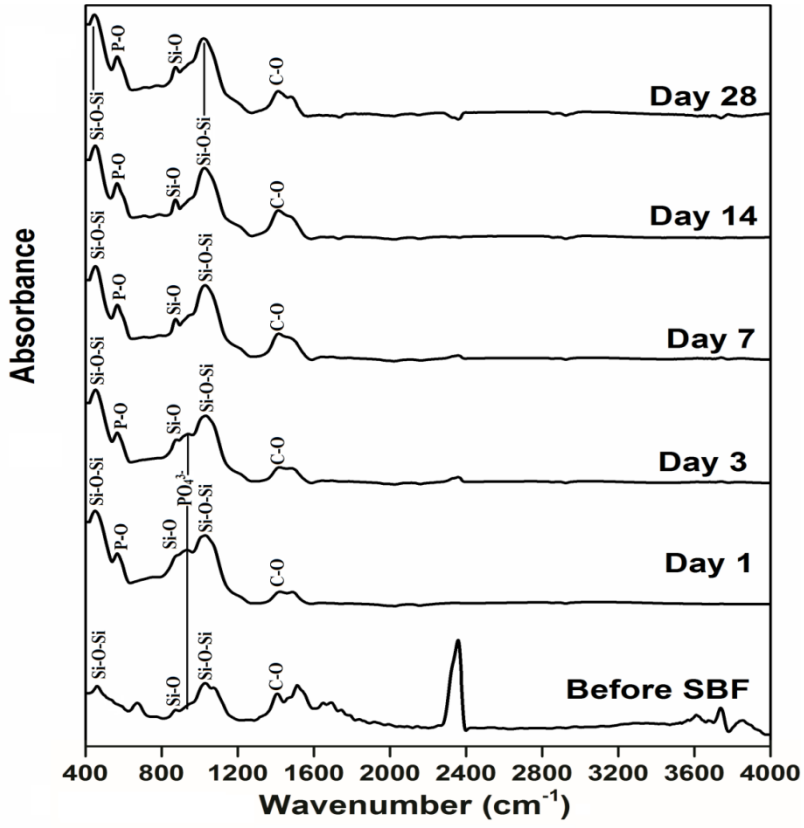

Fig. 4.9: FTIR absorption spectra of bioactive glass, K1 before and after soaking in SBF solution.

Fig. 9 shows the infrared spectral bands of K1 sample before and after immersion in SBF. The new bands were found to appear after 1 day immersion in SBF at around 567 cm^{-1} which correspond to P–O (phosphate) bending (Jastrzebski *et al*., 2011).

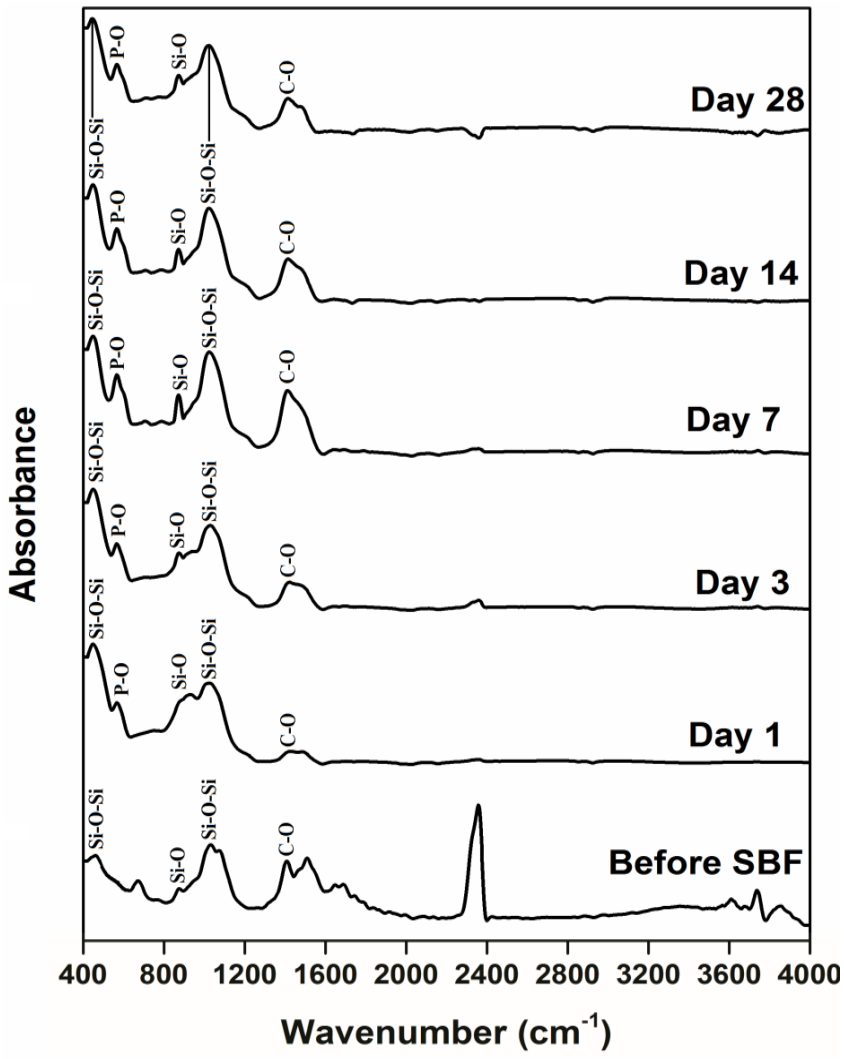

Fig. 4.10: FTIR absorption spectra of bioactive glass, K2 before and after soaking in SBF solution.

The bands corresponding to the frequencies of 1414 and 1644cm^{-1} are associated with C–O (carbonate) stretching mode and a minor peak at around 2358cm^{-1} as well as at 3023

cm^{-1} can be assigned due to the presence of O–H (hydroxyl) groups on the surface of the sample. The vibrational bands at around 935 cm^{-1} are attributed due to PO_4 (P–O stretching) groups (Figs. 4.9–4.11).

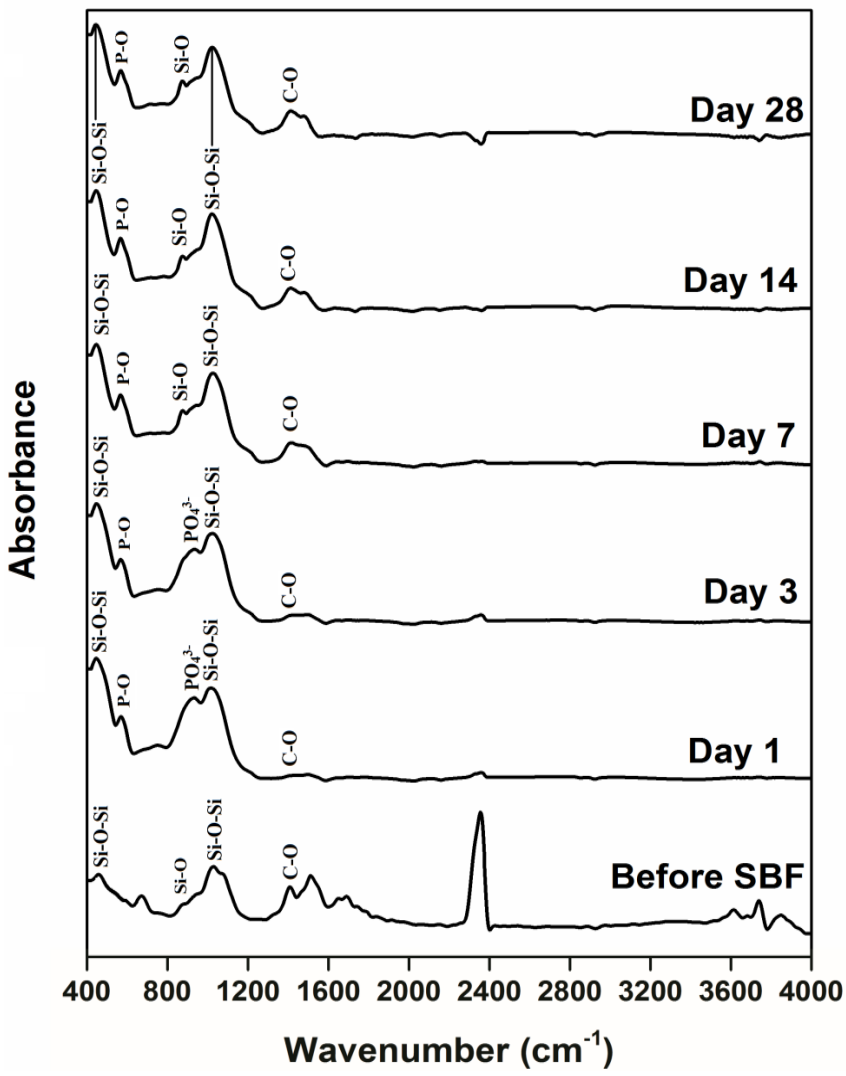

Fig. 4.11: FTIR absorption spectra of bioactive glass, K3 before and after soaking in SBF solution.

All the samples (K1–K5) are showing similar characteristics bands. The vibrational bands at around 450 cm^{-1} are due to Si–O–Si bending mode of vibrations or may be due to the

formation of AlO_6 octahedra in the SBF treated sample. However on increasing the concentration of alumina in the sample up to 2.5 mol% Al_2O_3, an additional band was found to appear at around 705 cm^{-1} which was attributed significantly due to the formation of AlO_4 tetrahedra in the sample after SBF treatment (Figs. 4.10–4.13).

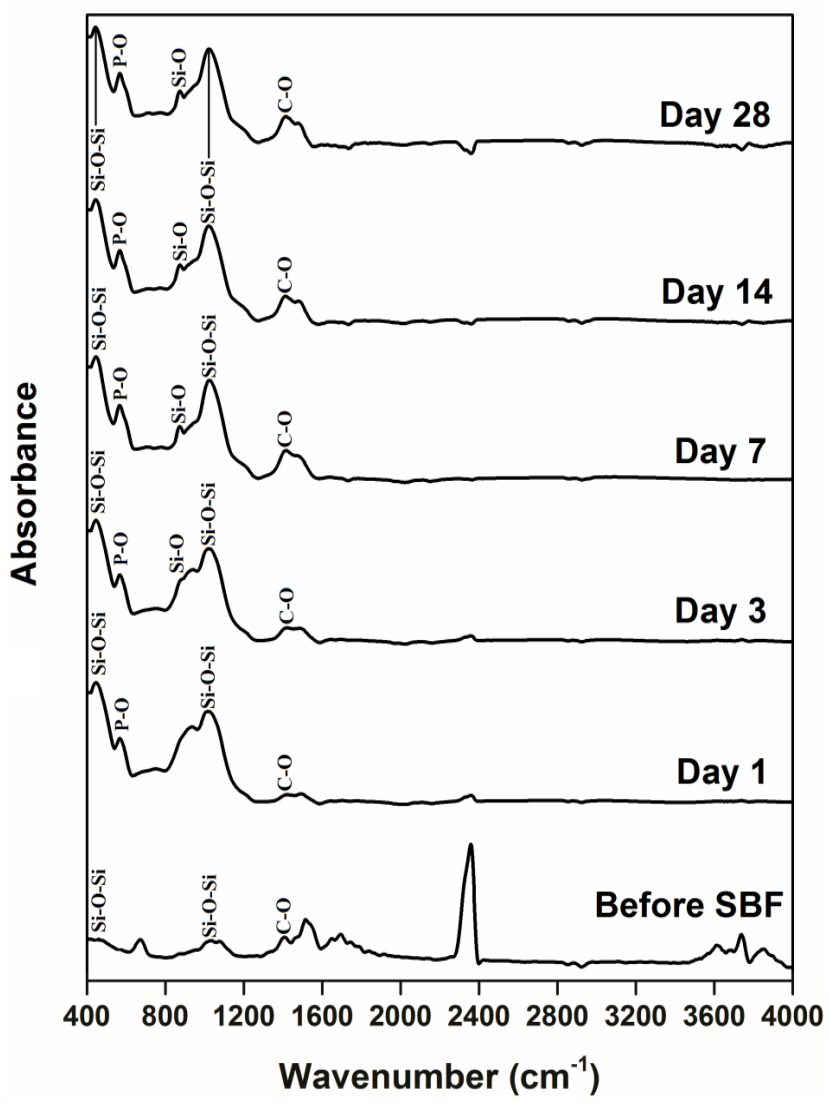

Fig. 4.12: FTIR absorption spectra of bioactive glass, K4 before and after soaking in SBF solution.

The results are also supported by Mohini *et al*. (Mohini *et al*., 2013) who had made similar observations regarding appearance of the FTIR bands at around 720 cm^{-1} and 476 cm^{-1} due to formation of AlO_4 and AlO_6 units in their SBF treated soda–lime–alumino–boro–phospho–silicate glasses. The prolonged period of treatment of the sample in SBF shows the similar behavior favorably due to the formation of hydroxyl carbonate apatite (HCA) layer.

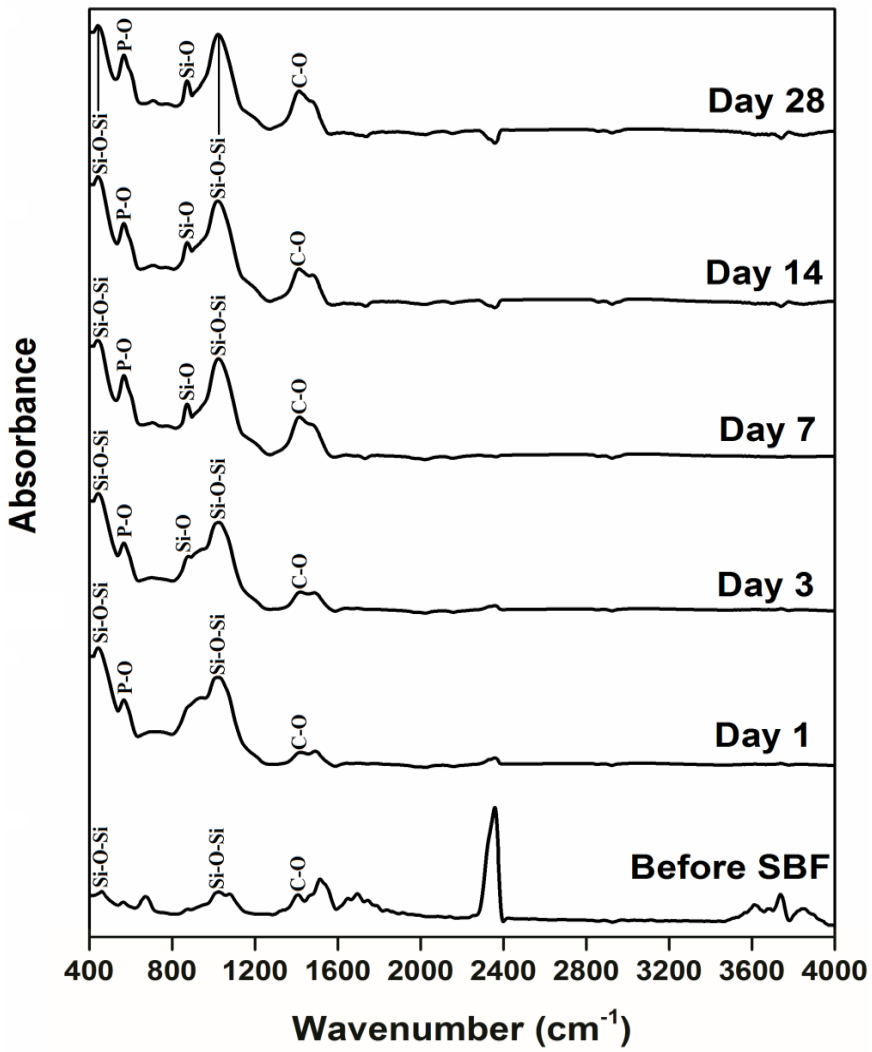

Fig. 4.13: FTIR absorption spectra of bioactive glass, K5 before and after soaking in SBF solution.

4.3.6 Measurement of cell viability, cytotoxicity and cell proliferation

We have performed cell viability and cellular proliferation studies for the bioactive glass samples (K1, K2, K3, K4 and K5) against human osteosarcoma cells U2-OS (Fig. 4.14). Bioactive glass sample (K1) is significantly less toxic compared to others as demonstrated by the inhibition of the cell viability in a time dependent kinetic study. Our results suggest that as the concentration of Al_2O_3 increases, the cell viability was significantly affected by K2, K3, K4 or K5 compared to K1 product ($P < 0.0001$ at concentration 100 μg/ml) (Fig. 4.14(A)). Viability of tumor cells only treated with complete medium alone was considered as 100%. The loss of cell viability was also supported by growth inhibition by bioactive glass samples when the U2-OS cells were cultured in presence of varying concentrations of the K2, K3, K4, and K5. K1 was found to be relatively less toxic compared to others in a concentration dependent manner in 48h MTT assay to assess the cell proliferation (Fig. 4.14(B)). Data suggest that, the cell proliferation was reduced to 30% in presence of K1 (at 48 h). Other bioactive glass samples cause significantly higher reduction in the proliferation of U2-OS cells (Fig. 4.14(B)). This was probably due to the increasing molar concentration in Al_2O_3 of samples K2, K3, K4 and K5 respectively.

K1 was also less cytotoxic to U2-OS cells compared to K2, K3, K4 and K5 at each concentration tested (Fig. 4.14(C)). Concentration dependent kinetic study indicates that at the lowest concentration (25 mg/ml), K1 is significantly less toxic compared to K2, K3, K4 and K5 ($P < 0.005$). At the highest concentration100 mg/ml, all the samples are toxic causing > 80% death of U2-OS cells (Fig. 4.14(C)). The cell viability and cytotoxicity data suggests that bioactive glass sample K1 is relatively tolerant to U2-OS

cells compared to other bioactive glass samples which causes significant loss of cell viability and direct cellular cytotoxicity.

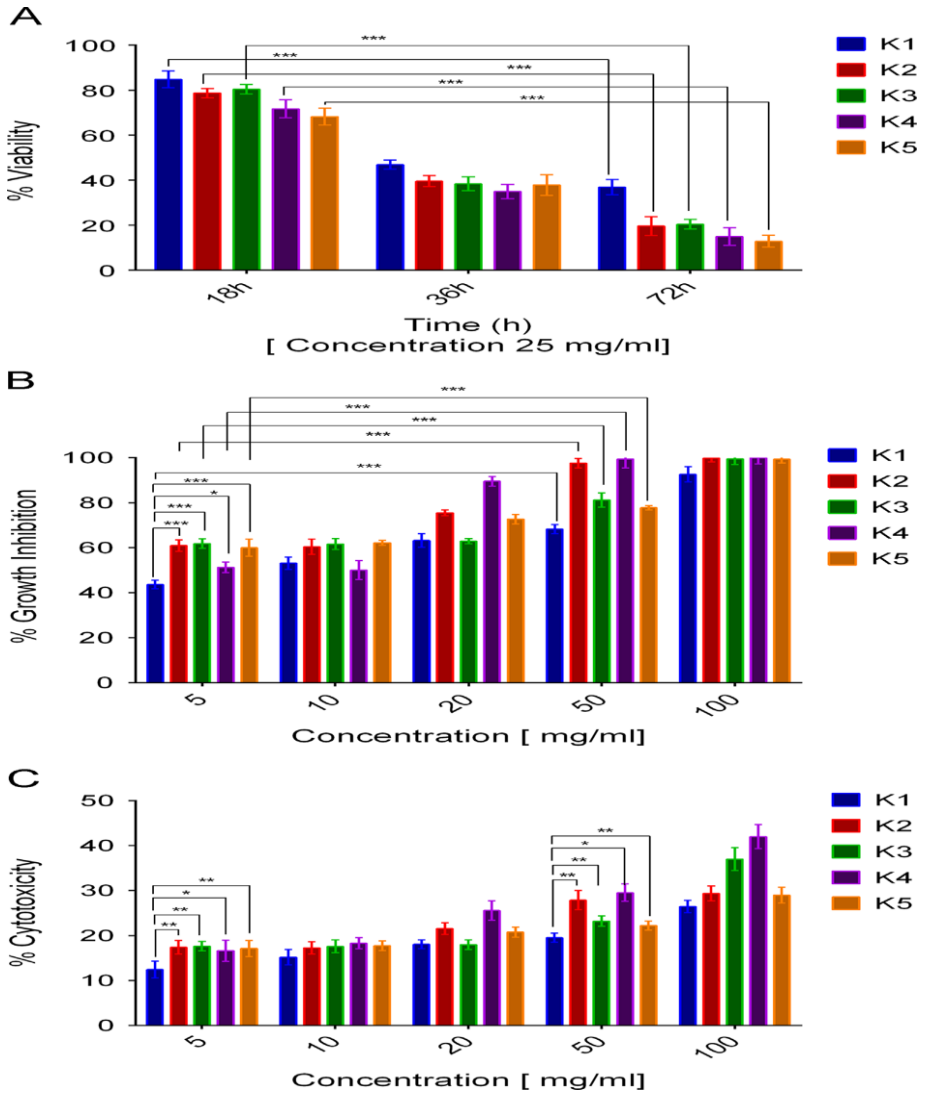

Fig. 4.14: Higher concentrations of bioactive glass sample inhibit osteosarcoma cells. (A)XTT Viability of U2-OS cells in presence of fixed concentration (25 mg/ml) of bioactive glass sample. (B) Anti-proliferative effect of increasing concentrations of bioactive glass sample against U2-OS cells assessed by MTT assay. (C) Direct cytotoxicity of U2-OS cells in presence of increasing concentrations of bioactive glass samples. Data presented as Mean ± SD with triplicate determination, n=3.

4.3.7 Effect on normal cells

In contrast to tumor cells, bioactive glass samples are tolerant to normal human RBC and PBMC. Bioactive glass samples do not cause hemolysis of RBC in a time dependent kinetic study using a fixed concentration of the samples (Fig. 4.15(A)).

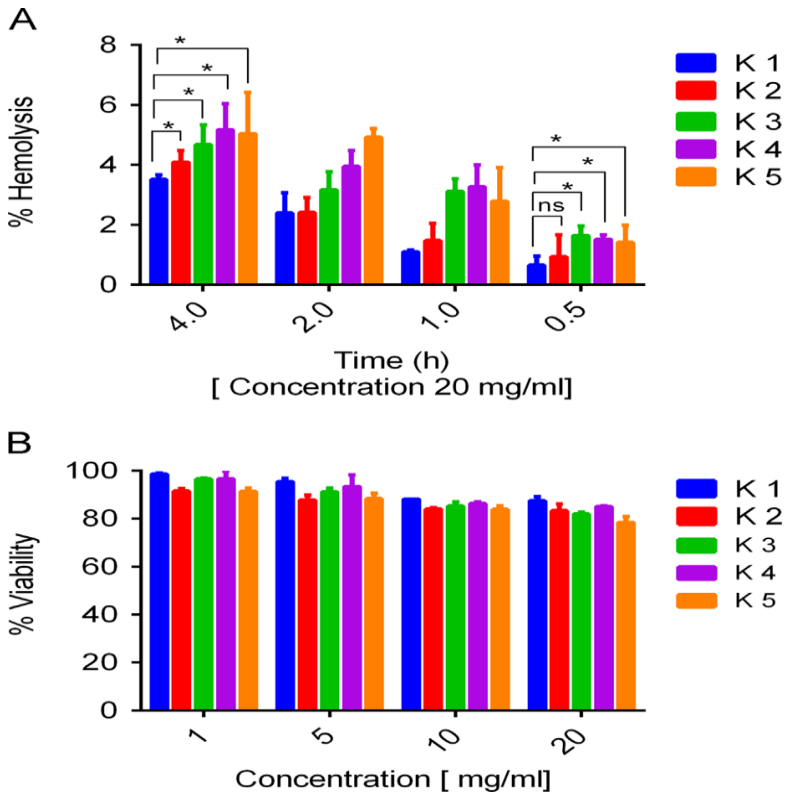

Fig. 4.15: Bioactive glass samples are tolerant to human RBC and PBMC. (A) Lack of hemolysis in RBC by bioactive glass samples in time dependent kinetic study. (B) Viability of PBMC was studied by XTT assay in presence varying concentrations of indicated samples. Mean ± SD, n=3.

The hemolysis rate never crossed above 5% for all the samples tested. K4 and K5 exhibit slightly higher hemolysis following incubation of RBC with the compound for 4h.

Normal human PBMC was also tolerated by bioactive glass samples and does not cause significant loss of viability at all the concentration tested, (Fig. 4.15(B)).

4.3.8 Induction of tumor cell apoptosis by bioactive glass samples

Broad spectrum growth inhibition by bioactive glass samples raises the question whether it also causes apoptosis of the tumor cells.

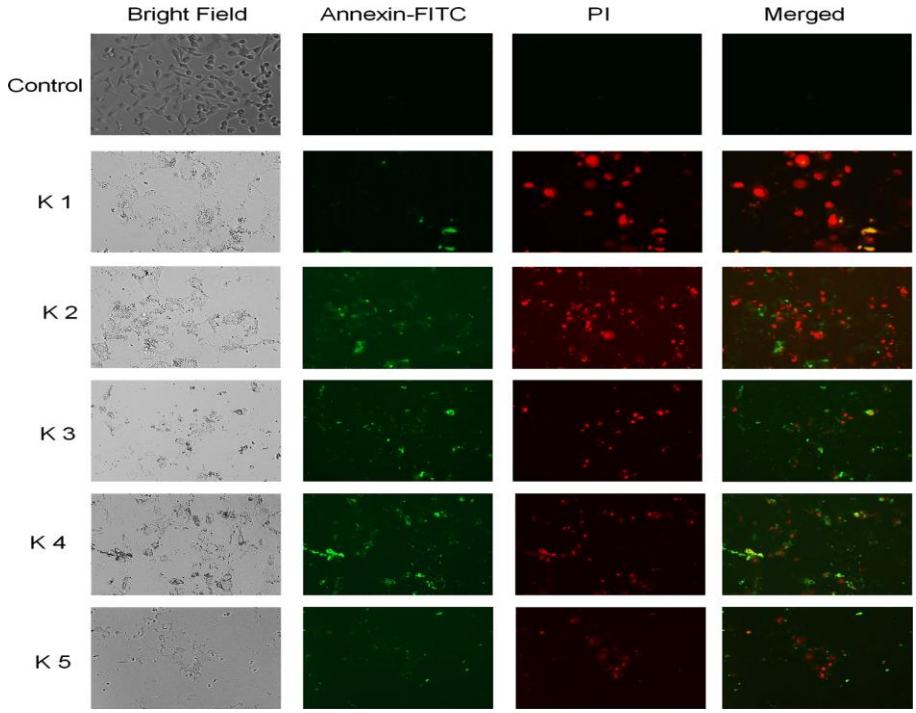

Fig. 4.16: Microscopic analysis of induction of apoptosis.U2-OS cells were given the indicated treatment with equivalent bioactive glass samples (25 mg/ml) in complete RPMI 1640 medium for 12 h at 37°C, 5% CO_2. The FITC-conjugated Annexin V and Propidium iodide (PI) stained apoptotic cells were visualized under a fluorescence microscope (Nikon Eclipse80i, Nikon, Japan) with Plan Fluor, 40x, NA 0.75 objective equipped with green and red filters for FITC and PI, respectively, n=4.

Apoptosis was determined by monitoring changes in the cell size and externalization of phosphatidylserine qualitatively in U2-OS cells. There was an abundance of Annexin V positive cells in U2-OS cells, treated with K3, K4 and K5. The sample K1 causes relatively less apoptosis as well as cell death as demonstrated by Annexin positivity and PI positive cells (Fig. 4.16).

4.3.9 Phagocytosis of bioactive glass samples by human macrophage

The studies on the phagocytosis of bioactive glass samples by the human macrophages were made. In a typical bone replacement scenario I could speculate that macrophages will be recruited in the areas of bone replacement in large numbers.

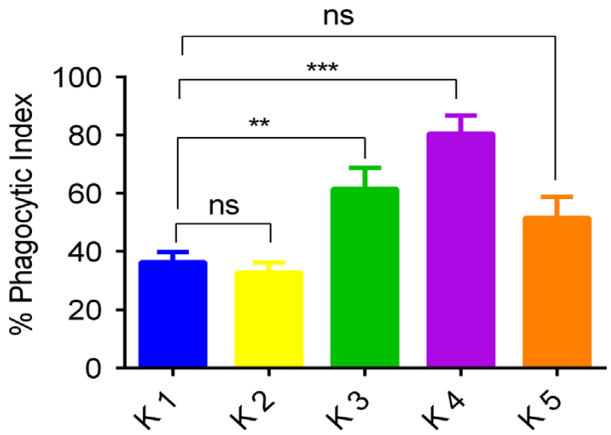

Fig. 4.17: Phagocytosis of bioactive glass sample by human macrophages. Human macrophages were cultured on glass cover slips in triplicate in complete medium at 37°C, 5% CO_2. The cells were incubated with bioactive glass samples (25 mg/ml) in complete medium for 24h. The cells were washed, fixed in ethanol and stained with Giemsa stain and observed under microscope. Intra cellular particles were counted and percent phagocytosis was calculated for each treatment. Mean ± SD, n=3.

As an important phagocytic cell, macrophage could be involved in eating of the bone ceramic materials leached following replacement. It was observed that bioactive glass samples are phagocytosed by the macrophages following 24 h of incubation with the macrophages (Fig. 4.17). Interestingly, K3, K4 and K5 demonstrate significantly higher phagocytosis compared to K1 or K2. Since K3, K4 and K5 are more toxic to the cells, macrophages might become more active in scavenging the compounds. This could be normal immune response to protect the body from deleterious effect of K3, K4 and K5 if any.

4.3.10 Culture of U2-OS cells on bioactive glass samples

I cultured the U2-OS cells on the bioactive glass samples in order to demonstrate the biocompatibility in case of clinical application. It was observed that K1 is most compatible with respect to growth of the U2-OS cells. K2 and K3 also supports the growth of U2-OS cells. Presence of Al_2O_3 in the bioactive glasses with increasing higher concentration makes the bioactive glasses less compatible with negligible number of cell's cellular growth on the surface of K4 and K5. This is compatible with the present results as observed with reference to growth inhibition and cytotoxicity as demonstrated in next page (Fig. 4.18).The present results suggest that, higher concentration of Al_2O_3 in glasses caused a cell death and retard the cell proliferation.

4.4 Conclusion

The present study with the SiO_2–CaO–P_2O_5–K_2O–Al_2O_3 based bioactive glasses suggests that the material could be used in bone replacement for clinical cases. The bioactive

glasses have demonstrated high degree of tolerance for the RBC and WBC which strongly supports its suitability as an alternative for bone replacement.

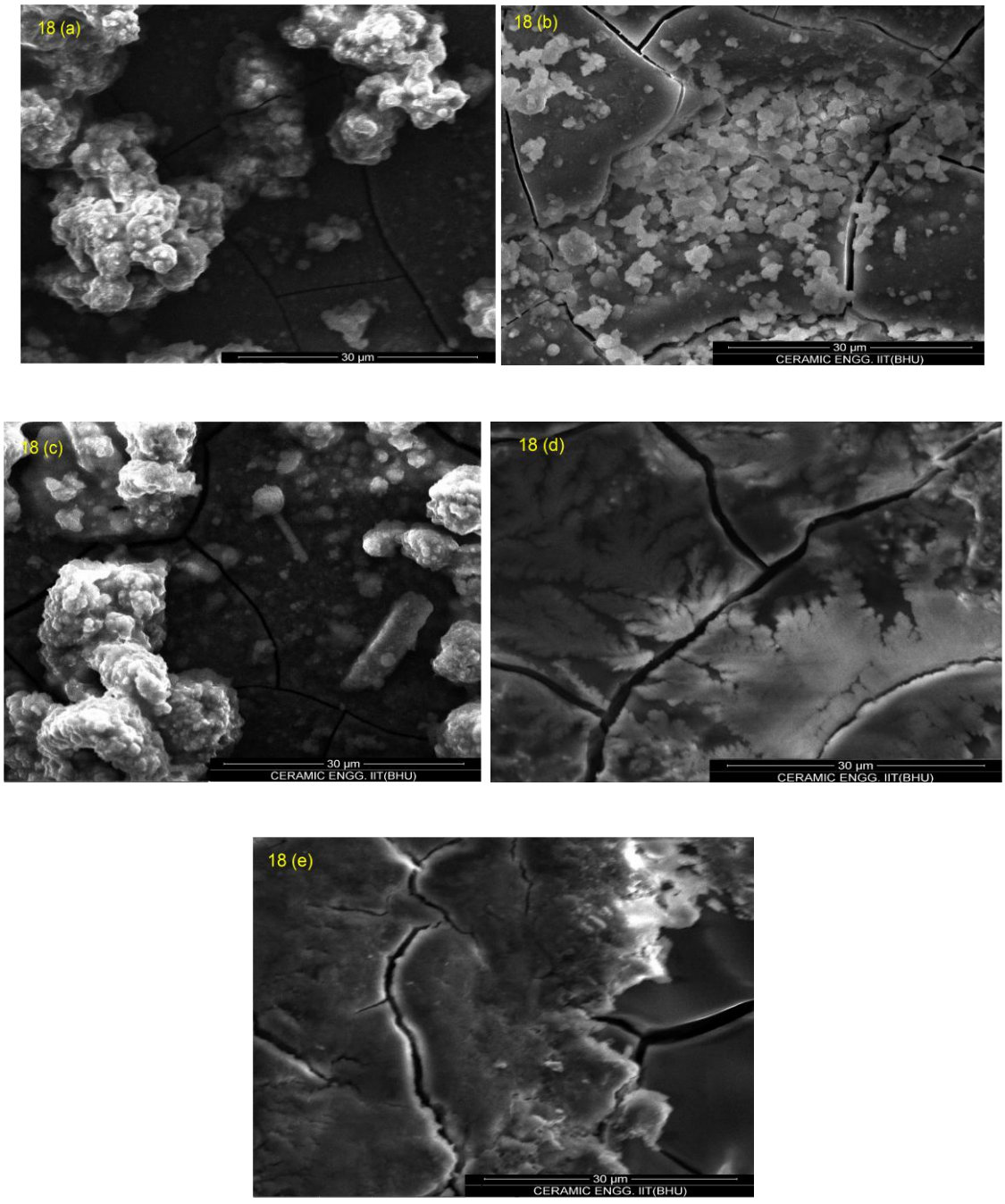

Fig. 4.18 (a-e): SEM micrographs of U2-OS cells growth on biocompatible glass samples (K1-K5).

Besides that U2-OS osteosarcoma cells were found to grow on samples K1, K2 and K3 efficiently suggesting its applicability as an implant material.

Higher molar concentration of Al_2O_3 in K4 and K5 causes cellular apoptosis and loss of viability in U2-OS cells although the other samples are relatively non-toxic. Based on the characterizations of the bioactive glass samples by XRD, FTIR, SEM and *in vitro* pH behavior the accommodation of these bioactive materials for bone replacement could be achieved as per modifications in molar ratios of Al_2O_3 which would make them biocompatible.

References:

Anderson OH, Liu G, Karlsson KH, Niemi L, Miettinen J and Juhanoja J, In vivo behavior of glasses in the SiO_2–Na_2O–CaO– P_2O_5–Al_2O_3–B_2O_3 system, J Mater Sci Mater Med 1, 219–227, 1990.

Agathopoulos S, Tulaganov DU, Ventura JMG, Kannan S, Karakassides MA and Ferreira JMF, Formation of hydroxyapatite onto glasses of the CaO-MgO-SiO_2 system with B_2O_3, Na_2O, CaF_2 and P_2O_5 additives, Biomaterials, 27, 1832-1840, 2006.

Belkebir A, Rocha J, Esculcas AP, Berthet P, Gilbert BZ and Gabelica, Structural characterization of glassy phases in the system Na_2O–Al_2O_3–P_2O_5 by MAS and solution NMR, EXAFS and vibrational spectroscopy, Spectro Acta, 55, 1323–1336, 1999.

Brow RK, Tallant DR, Structural design of sealing glasses, J. Non-Crys Solids, 222, 396–406, 1997.

Brovarone Vitale C, Verne E, Appendino P, Macroporous bioactive glass-ceramic scaffolds for tissue engineering, J Mater Sci Mater Med, 17, 1069–1078, 2006.

Cannillo V, Sola A, Potassium-based composition for a bioactive glass, Ceram Int, 35, 3389–3393, 2009.

Cao W, Hench LL, Bioactive Materials, Ceramics International, 22, 493–507, 1996.

Chengtie W, Ramaswamy Y, Kwik D, Zreiqat H, The effect of strontium incorporation into $CaSiO_3$ ceramics on their physical and biological properties, Biomaterials, 28, 3171–3181, 2007.

El-Kheshen A, Khaliafa FA, Saad EA, Elwan RL, Effect of Al_2O_3 addition on bioactivity, thermal and mechanical properties of some bioactive glasses, Ceramics International, 34, 1667–1673, 2008.

Fujiabayashi S, Neo M, Kim HM, Kokubo T, Nakamura T, A comparative study between in vivo bone in growth and in-vitro apatite formation on $Na_2O–CaO–SiO_2$ glasses, Biomaterials, 24, 1349–1356, 2003.

Filgueiras MR, LaTorre G and Hench LL, Solution effects on the surface reactions of three bioactive glass compositions, J Biomed Mater Res, 27 (12), 1485–1493, 1993.

Greenspan DC and Hench LL, Chemical and mechanical behaviour of bioglass coated alumina, J Biomed Mat Res, 10, 503–509, 1976.

Gross U and Strunz V, The interface of various glasses and glass ceramics with a bony implantation bed, J Biomed Mat Res, 19, 251–271, 1985.

Hanan H Beherei, Khaled R Mohamed and Gehan T El-Bassyouni, Fabrication and characterization of bioactive glass (45S5)/titania biocomposites, Ceramic International, 35, 1991-1997, 2009.

Hayakawa Satoshi, Tsuru Kanji, Ohtsuki Chikara and Osaka Akiyoshi, Mechanism of Apatite Formation on a Sodium Silicate Glass in a Simulated Body Fluid, J Am Ceram Soc, 82, 2155–2160, 1999.

Hench LL, Splinter RJ, Allen WC and Greenlee TK, Bonding mechanisms at the interface of ceramic prosthetic materials, J Biomed Mater Res, 334, 117–141, 1971.

Hench LL, Bioceramics, J Am Ceram Soc, 81, 1705–1728, 1998.

Hench LL and Polak JM, Third-generation biomedical materials, Science, 295, 1014–1017, 2002.

Hench LL, The story of bioglass, J Mater Sci Mater Med, 17, 967–978, 2006.

Huygh A, Schepers E, Barbier L and Ducheyne P, Microchemical transformation of bioactive glass particles of narrow size range, a 0–24 months study, J Mater Sci Mater Med, 13, 315–320, 2002.

Jastrzebski W, Sitarz M, Rokita M, Bułat K, Infrared spectroscopy of different phosphates structures, Spectrochim Acta PartA Mol Biomol Spectrosc, 79, 722–727, 2011.

Jones Julian R, Review of bioactive glass: from Hench to hybrids, Acta Biomater, 9, 4457–4486, 2013.

Kasuga Toshihiro, Hosoi Yoshimasa, Nogami Masayuki and Niinomi Mitsuo, Apatite Formation on Calcium Phosphate Invert Glasses in Simulated Body Fluid, J Am Ceram Soc, 84, 45-52, 2001.

Kim CY, Clark AE and Hench LL, Early stages of calcium-phosphate layer formation in bioglasses, J Non-Cryst Solids, 113(2), 195–202, 1989.

Kokubo T, Bioactive glass–ceramics properties and applications, Biomaterials, 12, 155–163, 1991.

Kokubo T, Kim HM and Kawashita M, Novel bioactive materials with different mechanical properties, Biomaterials, 24, 2161–2175, 2003.

Lashneva VV, Kryuchkov YN and Sokhan SV, Bioceramics based on aluminum oxide, Glass Ceram, 55, 357–359, 1998.

Le Geros RZ, Properties of osteoconductive biomaterials: calcium phosphates, Clin Orthop Relat Res, 395, 81–98, 2002.

Lin CC, Shen P, Chang HM and Yang YJ, Composition dependent structure and elasticity of lithium silicate glasses: effect of ZrO_2 additive and the combination of alkali silicate glasses, J Eur Ceram Soc, 26, 3613–3620, 2006.

Marti, Dr. Robert Mathys Foundation, Bischmattstr. 12, CH-2544 Bettlach, Inert bioceramics (Al_2O_3, ZrO_2) for medical application, Injury-international Journal of The Care of The INJURY-INT J CARE INJURED 01/2000; 31. DOI:10.1016/S0020-1383(00)80021-2.

Mohini G Jagan, Krishnamacharyulu N, Sahaya Baskaran G, Venkateswara Rao P and Veeraiah N, Studies on influence of aluminium ions on the bioactivity of B_2O_3–SiO_2–P_2O_5–Na_2O–CaO glass system by means of spectroscopic studies, Appl Surf Sci, 287, 46–53, 2013.

Muller D, Berger G, Grunze I, Ludwig G, Hallas E and Haubenreisser U, Solid state high-resolution 27A1 nuclear magnetic resonance studies of the structure of CaO-Al_2O_3-P_2O_5 glasses, Phys Chem Glasses, 24, 37–42, 1983.

Ohtsuki C, Kokubo T and Yamamuro T, Compositional dependence of bioactivity of glasses in the system CaO–SiO_2–Al_2O_3: it's in vitro evaluation, J Mat Sci Mat in Med, 3, 119–125, 1992.

Rehman I, Karsh M, Hench LL and Bonfield W, Analysis of apatite layers on glass–ceramic particulate using FTIR and FT-Raman spectroscopy, J Biomed Mater Res, 50(2), 97–100, 2000.

Schepers E, DeClercq M, Ducheyne P and Kempeneers R, Bioactive glass particulate material as a filler for bone lesions, J Oral Rehabil, 18, 439–452, 1991.

Sitarz M, Bulat K and Szumera M, Aluminium influence on the crystallization and bioactivity of silico-phosphate glasses from $NaCaPO_4$–SiO_2 system, J Non-Crystalline Solids, 356, 224–231, 2010.

Sitarz M, Structure and texture of glasses belonging to $KCaPO_4$–SiO_2 and $KCaPO_4$–SiO_2–$AlPO_4$ systems, Physics and Chemistry of Glasses Euro J Glass Sci & Tech, 51, 179–186, 2010.

Tylkowski M and Brauer DS, Mixed alkali effects in Bioglass® 45S5, J Non-Cryst Solids, 376, 175–181, 2013.

Verne E, DiNunzio S, Bosetti M, Appendino P, Vitale Brovarone C, Maina G and Cannas M, Surface characterization of silver-doped bioactive glass, Biomaterials, 26, 5111–5119, 2005.

Zhao Di, Huang Wenhai, Rahaman Mohamed N, Day Delbert E and Wang Deping, Mechanism for converting Al_2O_3-containing borate glass to hydroxy apatite in aqueous phosphate solution, Acta Biomater, 5, 1265–1273, 2009.